Chirality-Pure Carbon Nanotubes Show Distinct Complexation with Recognition DNA

Sequences

Fjorela Xhyliu, Geyou Ao*

Department of Chemical and Biomedical Engineering, Washkewicz College of Engineering,

Cleveland State University, Cleveland, Ohio 44115, United States

*Corresponding Author

Email address: g.ao@csuohio.edu

ABSTRACT

Pure-chirality single-wall carbon nanotubes (SWCNTs) that are non-covalently complexed with

recognition DNA sequences exhibit unique interaction behavior and hybrid stability in aqueous

environments. The complexation of DNA-wrapped SWCNTs was found to be a strong function

of both the DNA sequence and SWCNT chiral structure, highlighted by the distinct coating

displacement of the same recognition DNA sequence from a pair of (6,5) enantiomers by a strong

surfactant. A broad range of changes were observed for different DNA/SWCNT recognition pairs

with surfactant exchange including the increase in nanotube photoluminescence intensity in the

near-infrared (NIR) from 1.3 to 14.7-fold and time constants deduced from DNA displacement

kinetics ranging from 9 s to 230 s. A large time constant of 230 s and a relatively small 4.4-fold

increase in NIR emission intensity were obtained for the CTC₃TC-(7,6) hybrid highlighting the

vast potential of short DNA sequences for improved nanotube sorting and hybrid stability in

aqueous environments. Additionally, CTC₃TC-(7,6) was identified as the only hybrid to exhibit

1

an increase in NIR fluorescence intensity in serum-containing cell culture media among all samples tested. Our results demonstrated unique optical properties and hybrid stability of DNA/SWCNT recognition pairs, providing a foundation for developing applications of chirality-pure SWCNTs.

1. Introduction

Single-wall carbon nanotubes (SWCNTs) are multifunctional nanomaterials with exceptional optical, electronic, mechanical, and chemical properties and have been the subject of extensive studies involving both in vitro and in vivo interactions with chemicals [1-4] and biomolecules [5–9]. Recent advances in post-synthesis sorting of carbon nanotubes, such as the use of recognition sequences of single-stranded DNA (ssDNA) to effectively select pure-chirality SWCNT species with a defined chiral index (n, m), have provided a material foundation for creating new nanomaterial tools with well-defined properties for biological imaging, sensing, and therapeutic applications [8,10–14]. The highly predictable electronic structures and optical properties of chirality-defined SWCNTs, such as the distinct E₁₁ electronic transition of nanotubes, offer many advantages for biochemical sensing and imaging advancement [15]. Particularly, semiconducting SWCNTs fluoresce exclusively in the near-infrared (NIR) region between approximately 900 to 1600 nm, that has attenuated autofluorescence and deep tissue penetration, providing the ideal condition for high contrast fluorescence detection in biological media [16–19]. Pure-chirality SWCNTs can be further utilized as spectrally coded, multicolor fluorescent probes that can selectively and sensitively detect analytes in many applications, such as targeted sensing, ratiometric sensors, and multiplexed imaging [18–21]. In addition, pure-chirality SWCNTs promote advances in ultra-low dose, high efficiency nanomedicines showing more than ten-fold lower dose compared to that of as-synthesized SWCNT mixtures when utilized as a multifunctional imaging, sensing, and therapeutic agent [8,22]. More recently, pure-chirality SWCNTs have been demonstrated as promising nanomaterial hosts for organic color centers, an emerging class of synthetic quantum emitters with robust, tunable NIR optical functionality for advanced technological applications in biosensing and bioimaging, optoelectronics, and photonics [23–26].

In addition to offering a powerful method for selecting specific (n, m) species in polymer aqueous two-phase (ATP) systems [11,27–29], DNA-wrapped SWCNT hybrids (DNA-SWCNTs) formed by non-covalent complexation through multivalent π - π interactions [30] between the DNA bases and the nanotube surface have demonstrated many interesting properties. These include selective modulation of the nanotube photoluminescence (PL) [31,32], targeted detection of biomolecules and biological processes [8,21,33], and enhanced biocompatibility and stability in intracellular environments [34,35] that are highly dependent on the combination of DNA sequence and SWCNT chirality. The underlying structural basis for sequence-dependent properties of DNA-SWCNTs has been linked to the formation of ordered DNA wrapping structures on the nanotube surface providing unique surface functionalities for each purified hybrid [36–38]. The distinct binding of a DNA recognition sequence towards a specific (n, m) species, including enantiomers of a (n, m) SWCNT, can lead to a small difference in the solvation free energy of the hybrid, yet sufficient to differentiate the selected hybrid from a nanotube mixture in a ATP system that has slightly different physical properties [11,27,38,39].

The DNA binding to SWCNTs have been determined by many techniques through measuring interaction forces and thermodynamics of the hybrid to understand the unique structural and physical properties of DNA-SWCNTs. These include AFM studies of peeling DNA oligomers

from nanotube [40], fluorescence spectroscopy of DNA-SWCNTs upon reactions with O₂ and surfactants [31,41–43], absorption spectroscopy of DNA-SWCNTs with surfactant exchange [44– 46], and molecular dynamics simulations [37–39,47] and machine learning [28] approaches to elucidate and even predict the DNA coating structure on a nanotube. Among these techniques, kinetics of the DNA displacement by a surfactant through monitoring fluorescence spectral changes have been proven to be a fast and efficient way to probe the complexation affinity of a DNA sequence and SWCNT chirality. This is due to the highly sensitive nanotube PL as compared to its absorption, allowing detection of small perturbations in the external environment through measuring spectral changes of sharp emission peaks of (n, m) SWCNT in the NIR [41–43]. However, previous studies on kinetics of surfactant exchange of DNA coatings have been limited to either a synthetic SWCNT mixture comprised of a population of over thirty different (n, m) SWCNT species or a (6,5)-enriched SWCNTs complexed with a non-recognition ssDNA sequence. Although the binding affinities between ssDNA and SWCNTs have been quantitatively deduced in these studies, the interference of many (n, m) SWCNT species within a polydisperse molecular system and the random combination of DNA/SWCNT may diminish efforts in elucidating distinct interactions of DNA-SWCNT recognition pairs that yield unique optical and physicochemical properties for applications.

Here, we report the first comprehensive work on elucidating the distinct complexation of chirality-pure SWCNT and recognition ssDNA sequence by NIR fluorescence spectroscopy through measuring the DNA coating displacement by sodium deoxycholate (SDC), a surfactant known to bind strongly to nanotubes. A total of ten pure-chirality semiconducting (n, m) SWCNT species, including a pair of (\pm) (6,5) enantiomers, have been purified by our previously reported method using recognition DNA sequences in polymer ATP systems [11,29]. The polymer ATP

separation method allows us to purify sufficient quantities of nanotubes and perform a minimum of three repeats of each experiment described in this work. The spectral modulation of pure chirality (n, m) SWCNTs including spectral wavelength shifts and changes in spectral line width and emission intensity were monitored in aqueous environments. We treated kinetics of DNA displacement with single-exponential fits to changes in fluorescence emission intensity as a function of time upon surfactant exchange. Characteristic optical features, such as PL intensity increase and deduced time constants with surfactant exchange, were found to be unique to each DNA-SWCNT hybrid with no clear dependence on the DNA length and nanotube diameter. The role of (n, m) chiral structure on the DNA binding was further highlighted by displacing the same recognition DNA sequence from a pair of (6,5) enantiomers. In addition, changes in absorption and emission intensities of pure-chirality SWCNT species have been monitored in both serum-free and fetal bovine serum (FBS)-containing cell culture media. Purified DNA-SWCNTs showed relatively stable spectral features in serum-containing cell culture media than those exposed to serum-free media, providing potential of creating NIR optical probes with improved stability and specific functionality for biological applications. These findings provide better understandings of distinct complexation of DNA/SWCNT recognition pairs, offering important insights for developing effective nanotube sorting and stable optical nanoprobes for biochemical sensing and imaging applications utilizing pure-chirality SWCNTs. Representative spectroscopy findings are presented in the main text, but a substantial amount of experimental data is also included in the Supplementary Data.

2. Experimental

2.1. Preparation of pure-chirality (n, m) SWCNT species by DNA

Stock DNA-SWCNT dispersions and pure-chirality (n, m) species were prepared according to the previously published procedure [11,48]. Briefly, CoMoCAT SWCNT powders (SG65i-L39 and EG150-L670; CHASM Advanced Materials) were dispersed in a total volume of 1 mL aqueous solutions of recognition DNA sequences (Integrated DNA Technologies) containing 0.1 mol/L NaCl by tip sonication (model VCX 130, Sonics and Materials, Inc.) in an ice bath for 2 hours at a power level of 8 W. The SWCNT/DNA mass ratio was 1:2 with a fixed SWCNT concentration of 1 mg/mL. Supernatant dispersions were collected after 90 min centrifugation at 17,000 g for SWCNT purification. A total of ten (n, m) species including (7,3), (\pm) (6,5)enantiomers, (9,1), (8,3), (8,4), (7,6), (9,4), (11,1) and (10,3) were isolated in polymer aqueous two-phase (ATP) systems including 7.76 mass% poly(ethylene glycol) (6 kDa)/15.0 mass% polyacrylamide (10 kDa) (PEG/PAM) and 5.50 mass% PEG/7.50 mass% dextran (70 kDa) (PEG/DX) (Figure S1 and S2) [11]. The selection of recognition DNA sequences and details of SWCNT separation by polymer ATP method can be found in prior work [11,29]. Purified SWCNT species have diameters ranging from 0.706 to 0.936 nm [15] and an estimated number average length of 350 ± 100 nm [11]. Each (n, m) species is enriched in one of the handedness for chiral tubes, with (\pm) (6,5) tubes having the enantiomeric excess of > 90% for each handedness tube based on our previous report [11]. Here, the plus or minus sign of (6,5) species is assigned according to the signs of the circular dichroism values at the E_{22} position of (6,5) near 573 nm. Polymers were removed according to the SWCNT precipitation method reported previously [11,48,49]. Briefly, a final concentration of 0.5 to 1.0 mol/L sodium thiocyanate (NaSCN, Sigma-Aldrich) was added to purified (n, m) SWCNT species in polymer phases, and the sample was

incubated overnight at 4 °C. Adding the corresponding DNA recognition sequence at 100 µg/mL during the incubation stage is recommended to prevent nanotube aggregation. Then, the mixture was centrifuged at 17,000 g for 30 min to remove the solvent and the purified (*n*, *m*) SWCNT pellet was resuspended in deionized (DI) water by bath sonication at room temperature for 30 min. The corresponding DNA sequence at a final concentration of 100 µg/mL was added to purified SWCNT species to improve the dispersion stability for a long-term storage.

2.2. Displacing DNA coatings of nanotubes by a surfactant

A stock solution of 10 mass % sodium deoxycholate (SDC) (98 %, BioXtra) was prepared for DNA/surfactant replacement experiment at room temperature. The concentration of purified (n, m) SWCNT species was adjusted to an absorbance of 0.3 ± 0.02 at its E_{11} peak wavelength for surfactant exchange experiment, which corresponds to approximately a nanotube concentration of 1.65 µg/mL [50]. The complexation affinities of purified DNA-SWCNT hybrids in aqueous surfactant solutions were examined by three repeats using a total volume of 120 µL for each nanotube sample. Roughly 5 s after the initial measurement of DNA-SWCNT fluorescence, small aliquot of 0.6 µL stock SDC solution were added to DNA-SWCNT samples and mixed immediately to obtain a final concentration of 0.05 mass % SDC.

2.3.Incubation of purified DNA-SWCNTs in cell culture media

Purified (*n*, *m*) SWCNT species were incubated in GibcoTM RPMI 1640 Medium (Catalog No. 11-875-085, FisherScientific) containing 10 % (v/v) fetal bovine serum (FBS, Corning) at pH 7.54 for up to 8 hours in dark at room temperature, unless indicated otherwise, to monitor the

dispersion stability of purified DNA-SWCNT hybrids in cell culture media. Cell culture medium without FBS showed pH 8.3-8.4 during the 8 hour incubation. The optical spectroscopy of purified DNA-SWCNT hybrids in cell culture media was examined by three repeats. Small aliquots of 1-4 μ L of concentrated, purified SWCNT samples were added to a total volume of 120 μ L cell culture media with and without serum to obtain an absorbance value of 0.3 \pm 0.02 at the E₁₁ peak wavelength of SWCNTs (i.e., approximately 1.65 μ g/mL tubes).

2.4. Optical characterization of purified DNA-SWCNTs

Spectroscopy characterization including vis-NIR absorbance and near-infrared (NIR) fluorescence measurements were performed on a NS3 NanoSpectralyzer (Applied NanoFluorescence, LLC) using a 10 mm path length quartz cuvette. Fixed excitation wavelengths of 532 and 641 nm lasers, corresponding to E₂₂ peak positions of (*n*, *m*) species, were used for acquiring NIR fluorescence spectra. DNA displacement kinetics were monitored using sequence mode data acquisition through time-resolved fluorescence spectra at room temperature at a final concentration of 0.05 mass % SDC. MATLAB R2018b software was used for exponential fitting of DNA displacement kinetics.

3. Results and discussion

3.1.Preparation and optical characterization of DNA/surfactant exchange for pure-chirality SWCNTs

The structural diversity of SWCNTs produces a family of cylindrical carbon allotropes, where each (n, m) species exhibits unique optical and physicochemical properties for a wide range of applications, such as biochemical sensing and imaging. Separation of a pure-chirality (n, m)SWCNT with well-defined diameter, chiral angle, and electronic structure from their synthetic mixture is generally considered as a prerequisite for many applications. We isolated a total of ten pure-chirality (n, m) species using recognition DNA sequences by a polymer ATP separation method [11,27]. The corresponding absorbance and fluorescence spectra of purified DNA-SWCNTs clearly showed optical transition peaks of (n, m) species, such as E_{11} and E_{22} with little to no contribution from any other species (Figures S1 and S2). In addition to providing a source of chirality-pure nanotubes, purified DNA-SWCNT hybrids with ordered DNA folding structures exhibit vast potential as stable, biocompatible fluorescent probes to detect targeted biological interactions in the NIR [8]. It is important to utilize pure-chirality SWCNTs, as opposed to a synthetic SWCNT mixture, to study fundamental interaction behaviors of DNA/SWCNT recognition pairs. The interaction behavior of non-recognition DNA sequences with SWCNTs is not within the scope of this work.

The recognition DNA sequence forms an ordered wrapping structure in a single layer along the specific (*n*, *m*) SWCNT, creating different DNA coverages on the surface of nanotube (i.e., relating to the DNA density on tubes). However, the difference in the DNA coverage should not affect the complexation of recognition pairs of DNA and SWCNT investigated by DNA/surfactant

exchange [42]. We displace DNA coatings on a purified (n, m) species by adding a final concentration of 0.05 % SDC and directly measure spectral changes of both absorbance and fluorescence of nanotube samples at equilibrium (Figure 1). The concentrations of SDC and nanotubes used give a mass ratio of $\approx 300:1$ for SDC: (n, m) SWCNT, leading to the full displacement of DNA by excess SDC [44]. The absorbance spectra of nanotube samples showed varied spectral shifts (< 9 nm) to shorter wavelengths at the E_{11} peak of different (n, m) species, which is expected when displacing DNA with a strong surfactant (Table S1). Absorbance values at E_{11} remained relatively stable upon complete DNA displacement by SDC at equilibrium, an example of which is shown for CTTC₃TTC-(9,4) hybrid (Figure 1b). In comparison, spectral variations in nanotube emission after surfactant exchange, including intensity increase, narrowing of line width, and blue shift (i.e., decrease in wavelength) of the E_{11} peak of (n, m) species, showed large differences for different recognition pairs of DNA-SWCNTs (Table S2 and S3).

It is known that the excitonic optical transition energies of SWCNTs are influenced by the environmental effect such as coating materials and solvents providing different local dielectric properties surrounding nanotubes [51–53]. Changes in the environmental dielectric constant modulate the dielectric screening of excitons, leading to spectral changes of electronic transitions including solvatochromic shifts (i.e., spectral shift), changes in spectral width, and emissive quantum yields. Particularly, we observed a broad range of increase in nanotube PL intensity from 1.3-fold for $TTA(TAT)_2ATT$ -(-) (6,5) to 14.7-fold for $CTTC_2TTC$ -(8,3) hybrid with surfactant exchange. For example, fluorescence spectra of (9,4) species show that the E_{11} emission of SDC-coated (9,4) is significantly brighter with 12.8-fold increase in intensity, has a 6 nm decrease for the full width at half maximum (FWHM), and is blue-shifted by ≈ 7 nm, corresponding to the energy difference of 6.4 meV, compared with that of DNA-coated (9,4) (Figure 1c). These spectral

changes demonstrate the sensitivity of nanotube PL to its surrounding environment where the complete displacement of DNA coatings by SDC leads to changes in the local dielectric constant. The observed fluorescence enhancement after DNA/SDC exchange could be due to the improved, uniform surface coverage by SDC, shielding nanotubes from the surrounding solution [53]. In addition, the pH of purified DNA-SWCNT samples prepared in water remained relatively stable during the short time period of surfactant exchange experiments. Consequently, we utilized fluorescence spectra to analyze kinetics of DNA displacement for all (*n*, *m*) SWCNT samples in water.

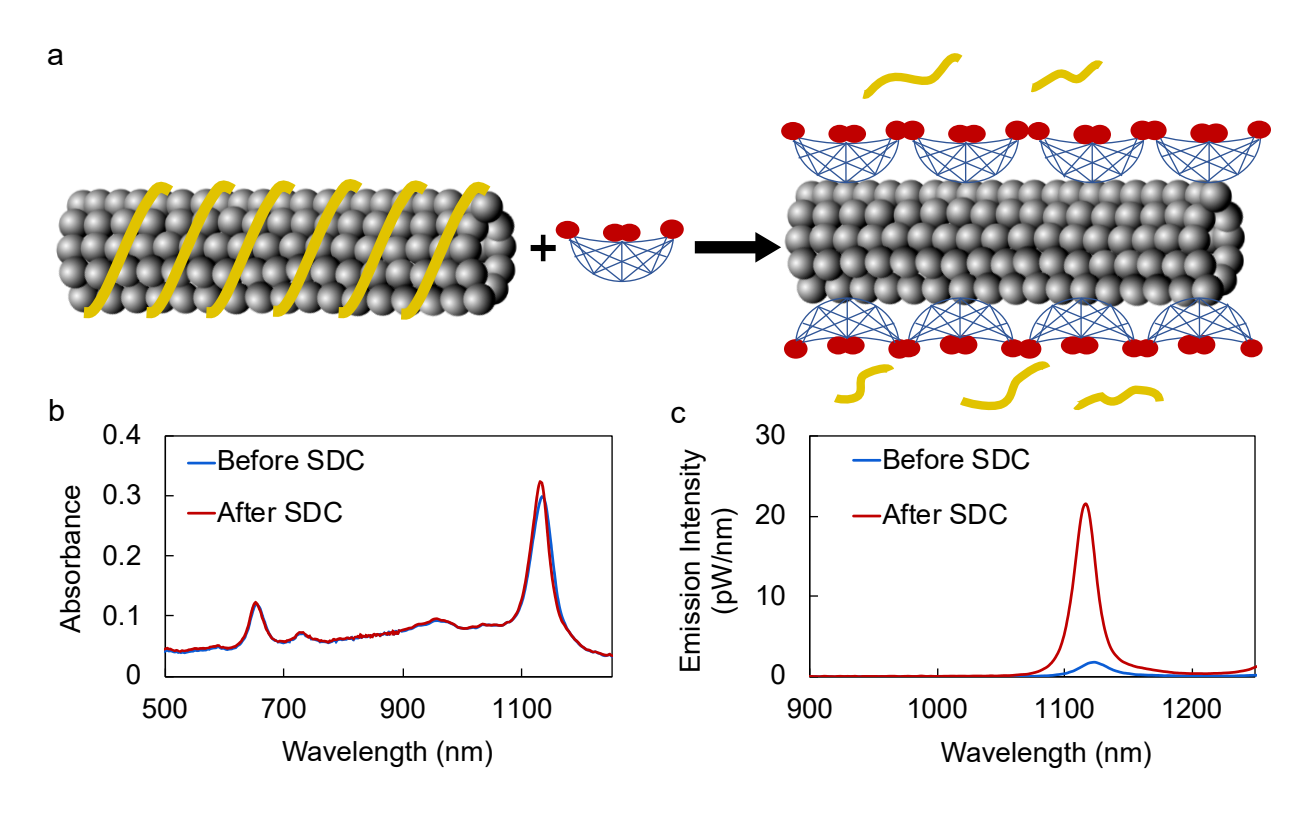


Figure 1. Schematic of DNA/SDC exchange process and corresponding optical characterization of purified CTTC₃TTC-(9,4) species. (a) Displacement of DNA surface coating on a nanotube by

SDC. (b) Absorbance and (c) fluorescence spectra for purified (9,4) species before and after adding SDC at equilibrium.

3.2. Kinetics of DNA displacement of pure-chirality SWCNTs by a surfactant

Because pure-chirality SWCNTs were employed, the evolving fluorescence spectra with time allowed us to extract defined spectral characteristics of the E_{11} emission peaks of (n, m)nanotubes to build simple kinetic models of DNA coating displacement. An example is shown for T₄C₄T₄-(11,1) enriched species in Figure 2. Clearly identifiable spectral modulations in emission intensity, line width, and peak position can be observed as DNA coatings being displaced by SDC. Interestingly, although (9,4) and (11,1) species have the same tube diameter, they showed distinct optical properties due to different surface coverage of molecules. Specifically, the E₁₁ emission intensity of (11,1) species gradually increased up to 10.9-fold accompanied by a significant narrowing of spectral line width with a decrease of ≈ 29 nm for FWHM and a blue shift of 14 nm (i.e., the energy difference of $\Delta E_{11} \approx 11.2$ meV) upon displacing DNA from nanotubes (Table S2 and S3). The large decrease in spectral line width observed for this hybrid may be due to the contamination of (10,3) species, resulting in a broader E₁₁ peak for the initial T₄C₄T₄-(11,1) sample (Figure S1). Regardless, we observed these combined optical phenomena of the brightening of nanotube PL, the narrowing of line width, and the blue shift in E₁₁ peak wavelength for the majority of SWCNT samples as the surface structures transition from DNA-wrapped coatings, DNA conformational change and displacement by SDC to an improved surface coverage by SDC coatings. An exception is observed for the CTTC₂TTC-(8,3) hybrid, which did not show an apparent wavelength shift despite the 14.7-fold increase in E₁₁ emission intensity and a narrower spectral shape for SDC-coated SWCNT (SDC-SWCNT). Because consistent increase in emission

intensity was obtained for each (n, m) species with clearly identifiable optical transition peaks within the experimental time period, we analyzed kinetics of DNA coating displacement by investigating the change in emission intensity at the E_{11} peak wavelength of SDC-SWCNTs as a function of time.

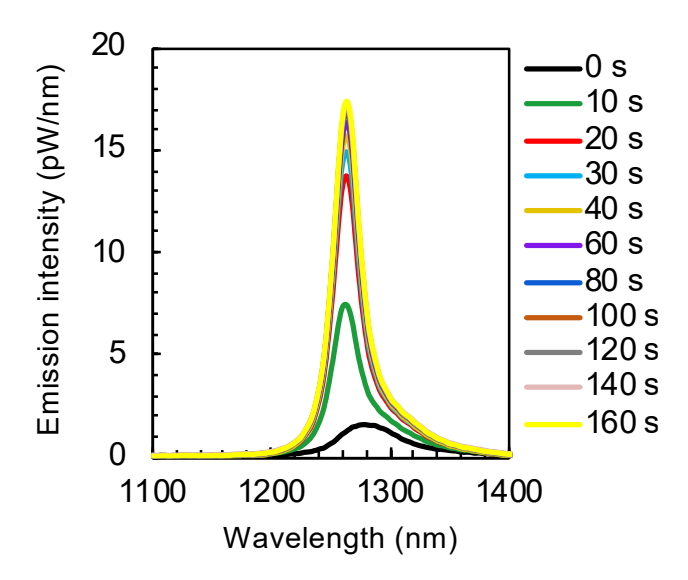


Figure 2. Time-resolved fluorescence spectra for purified T₄C₄T₄-(11,1) species showing distinct spectral changes in the E₁₁ emission peak during DNA displacement by SDC. Samples were excited at 641 nm.

Each purified (n, m) SWCNT exhibits clear E_{11} emission peak during DNA displacement by surfactant. Figure 3 plots the time dependence of emission intensity ratio I/I_O of nanotubes at the E_{11} peak wavelengths of (n, m) SWCNTs, where I and I_O are the magnitude of emission peaks corresponding to SDC- and DNA-coated (n, m) SWCNTs. The time traces of increase in intensity ratio for all SWCNT samples can be modeled using single exponential fit (Table S4, $R^2 > 0.9$ for all fits from three repeats). This suggests that our surfactant exchange reaction operates as a pseudo-first order reaction as proposed for prior studies on ssDNA displacement kinetics using SWCNT mixtures [41,42,44]:

$$DNA-(n, m) SWCNT + SDC \xrightarrow{k} SDC-(n, m) SWCNT + DNA$$

where k is the rate constant corresponding to the inverse time constant 1/t obtained from the exponential fit.

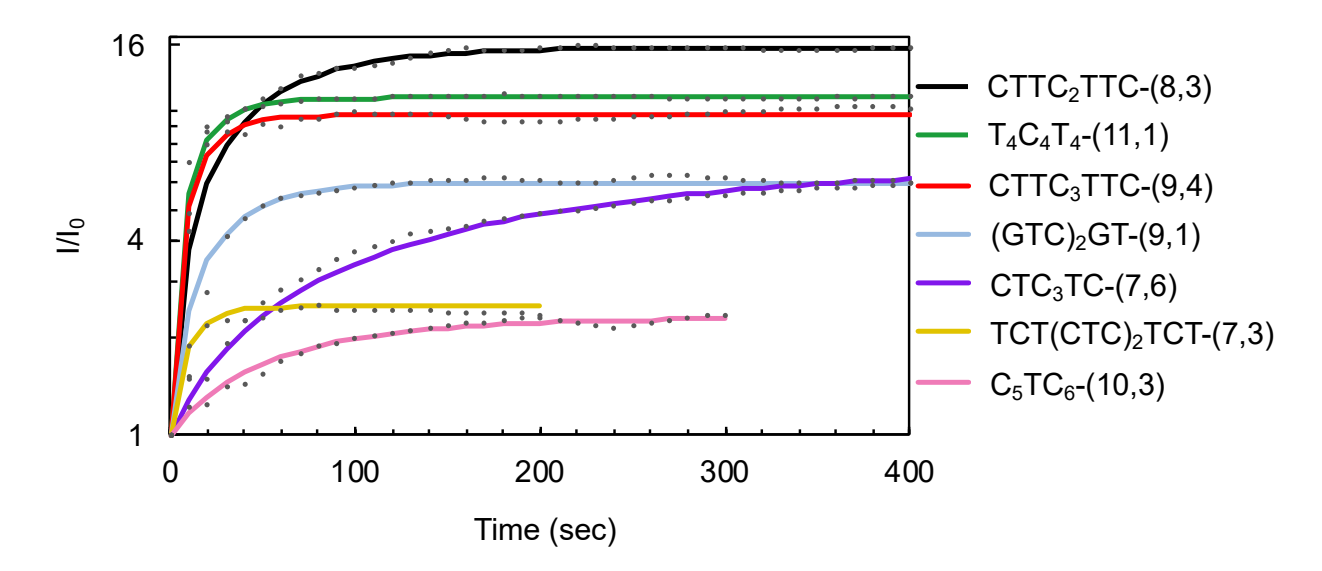


Figure 3. Measured (dotted lines) and exponential fits (solid curves) of fluorescence kinetics for purified DNA-(n, m) SWCNT samples during SDC exchange showing distinct responses in intensity ratio change for each (n, m) species at the E_{11} peak wavelength of nanotubes coated by SDC.

3.3. Comparison of distinct DNA displacement kinetics for (6,5) enantiomers

Additionally, we tested a pair of (6,5) enantiomers that are coated with the same recognition sequence $TTA(TAT)_2ATT$ to demonstrate the importance of (n, m) chiral structure on

the interaction of nanotubes with DNA. Because of the difference in coating structure of the same DNA on the two enantiomers, kinetics of surfactant exchange showed different behaviors for the two (6,5) samples (Figure 4). Specifically, (+) (6,5) showed a smaller blue shift of nearly 5 nm, a slightly larger increase in emission intensity (1.6-fold vs. 1.3-fold), and a shorter time constant (\approx 19 s vs. \approx 52 s) compared with that of (-) (6,5) sample. These indicate that the hybridization affinity of the recognition DNA sequence is stronger for the (-) (6,5) than its mirror image (+) (6,5). The observed difference in DNA displacement kinetics by a surfactant for (6,5) enantiomers suggests that different enantiomeric forms of the same (n, m) species may induce drastic differences in interactions between SWCNTs and various molecules of interest. This has potential implication in developing optical probes for detecting chiral molecules.

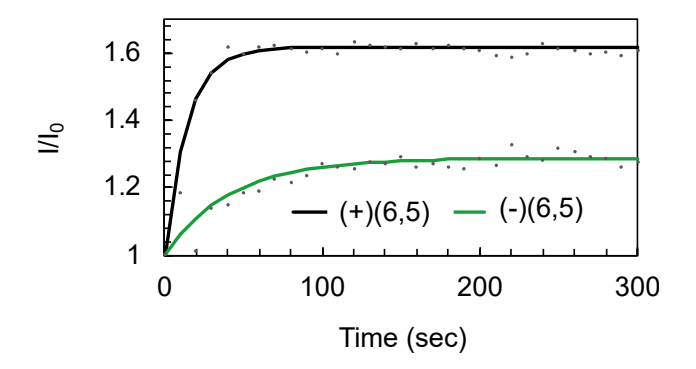


Figure 4. Fluorescence kinetics for purified (\pm) (6,5) enantiomers during displacement of the same TTA(TAT)₂ATT coating by SDC showing different responses in intensity ratios at the E₁₁ peak position of SDC- (\pm) (6,5). Dotted lines are experimental points and solid curves indicate the exponential fits for each enantiomer.

3.4. Analysis of spectral changes in E_{11} emission peaks of nanotubes with surfactant exchange

The distinct SWCNT chirality determines the diameter, chiral angle, and electronic structure of each (n, m) species. We plotted average spectral changes in E_{11} emission peaks of DNA-SWCNT recognition pairs after adding SDC as a function of nanotube diameter (d) and chiral angle (θ) , respectively, indicating mod (n-m, 3) = 1 and mod (n-m, 3) = 2 semiconducting nanotubes [15] (Figure 5 and Figure S3). Table S3 summarizes values corresponding to spectral changes that are obtained from three repeats. Metallic tubes that do not emit PL and have mod (n-m, 3) = 0 are not considered for this study. A broad range of PL intensity increase (i.e., I/I_O) from 1.3 to 14.7-fold was obtained for purified DNA-SWCNT hybrids tested, however no obvious correlations with either nanotube diameter or chiral angel were observed. Similarly, we did not observe obvious pattern for changes in spectral wavelength shift ($\Delta\lambda_{11}$), energy shift (ΔE_{11}), and line width (Δ FWHM) as a function of diameter and chiral angel, respectively, for each (n, m)species tested. This suggests that either diameter or chiral angle of nanotubes alone cannot account for spectral changes when displacing DNA coatings by surfactant. In addition, we considered the chirality effect of nanotubes on PL intensity ratios of DNA-SWCNT hybrids after surfactant exchange, but no obvious pattern was observed (Figure S4). The absence of clear dependence of spectral changes on nanotube chirality for DNA/SDC exchange suggests the unique complexation of recognition DNA sequence and specific SWCNT species.

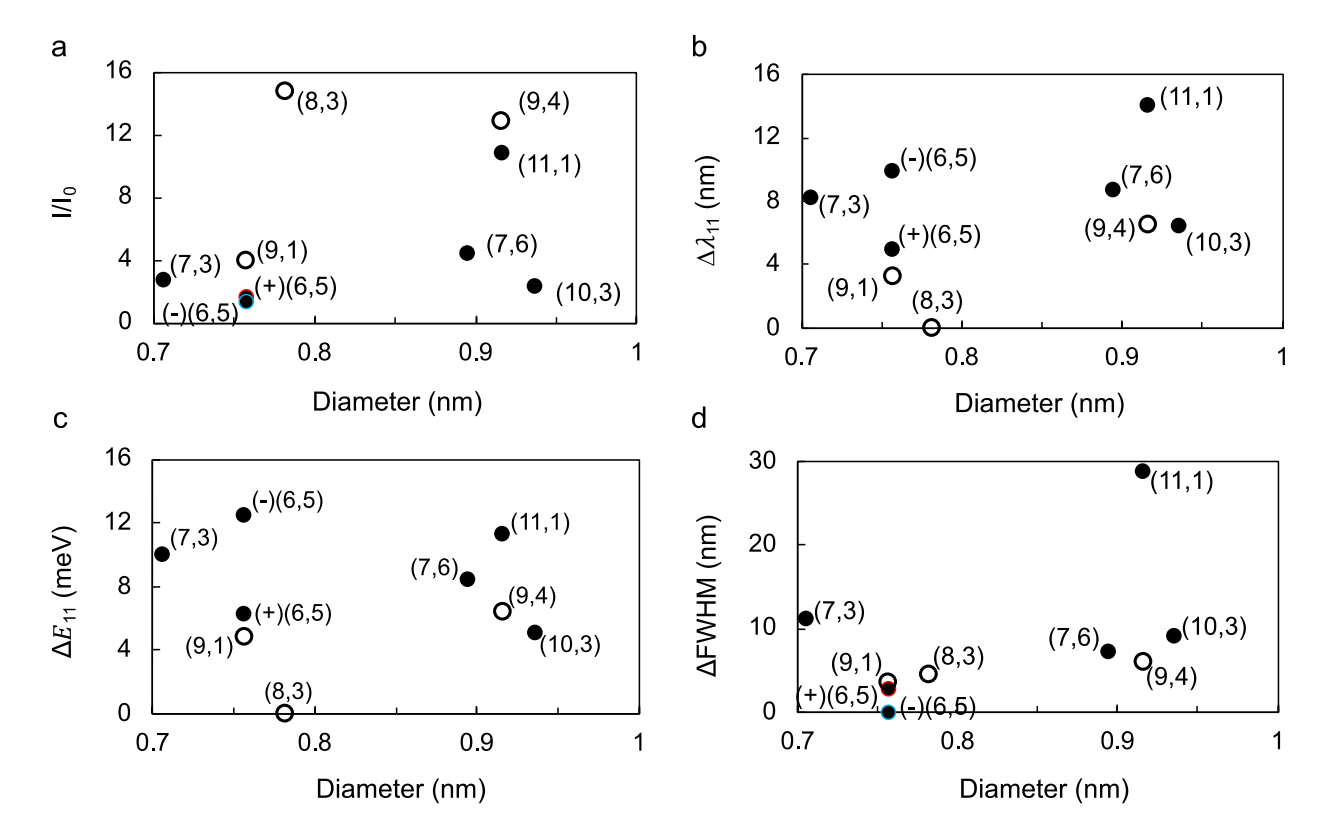


Figure 5. Spectral changes of E_{11} emission peaks of purified (n, m) SWCNT species as a function of nanotube diameter after DNA/SDC exchange at equilibrium. (a) PL intensity ratio increase, (b) wavelength and (c) energy shift, and (d) narrowing spectral line width of (n, m) species. Closed and open circles indicate mod 1 and mod 2, respectively.

We compared the interaction behavior of DNA sequences and SWCNTs based on the time constant obtained from spectral fit, where a longer time corresponds to a stronger binding affinity of the recognition DNA sequence to a (n, m) species (Figure S5) [42]. We observed significant differences in deduced time constants among DNA-SWCNT recognition pairs with roughly 25-fold increase from ≈ 9 s for TCT(CTC)₂TCT-(7,3) up to ≈ 230 s for CTC₃TC-(7,6) hybrid (Table S4). Among the (n, m) SWCNT species tested, (6,5) and (9,1) tubes have the same diameter of 0.757 nm, while the diameter of (9,4) and (11,1) tubes is 0.916 nm [15]. Although similar values

were obtained for (9,4) and (11,1) tubes, the deduced time constants of purified DNA-SWCNT hybrids showed no clear correlation to the nanotube diameter (Figure S5). Previously, larger time constants were observed for longer DNA length when dispersing SWCNT mixture samples using 6-mer to 60-mer ssDNA sequences [42]. However, DNA length is found to be not a factor affecting the time constants in our work as we utilized short recognition sequences of 7-mer to 12-mer. In fact, the stable CTC₃TC-(7,6) hybrid is complexed with the shortest DNA length (7-mer) tested, demonstrating the potential of short sequences for achieving improved nanotube sorting and stability of DNA-SWCNT hybrids in aqueous environments.

Pure-chirality DNA-SWCNT hybrids used in this work were separated in polymer ATP systems where the partition of the hybrid between the two phases is driven by the small difference in the surface functionality (i.e., the solvation free energy of the hybrid) [27,29]. It was proposed that the solvation free energy of a DNA-SWCNT hybrid is sensitive to the exact spatial distribution of hydrophilic groups (i.e., sugar-phosphate backbone of DNA that is exposed to water) along the nanotube axis, which is directly related to the wrapping pattern of DNA on the nanotube surface. Molecular dynamics simulations [28,38] of recognition pairs of DNA and SWCNT showed an ordered wrapping structure of the DNA sequence on the SWCNT chirality, which leads to the differentiation of its solvation energy by the ATP system from all other DNA/SWCNT combinations. Our data provide quantitative comparisons of the complexation of recognition DNA sequence and specific SWCNT species, however, the elucidation of underlying structural differences in the ordered structure of each DNA-SWCNT hybrid will benefit from computational work in future studies. Regardless, the relatively low PL intensity increase, and longer time constants obtained for CTC₃TC-(7,6) with surfactant exchange suggest improved surface coverage of DNA coatings on the nanotube as well as a stronger hybridization affinity of the hybrid.

Additionally, this CTC₃TC-(7,6) hybrid highlights the potential of short DNA sequences for separating and stabilizing pure-chirality nanotubes in aqueous environments.

3.5. Optical characterization of purified DNA-SWCNTs in cell culture media

Recent studies utilizing the purified CTTC₃TTC-(9,4) hybrid showed that pure-chirality SWCNTs exhibit long-term biocompatibility [8,34]. In addition to surfactant solutions, we characterized optical properties of purified DNA-SWCNT hybrids in cell culture media with and without serum. We identified CTTC₃TTC-(9,4) as one of the two hybrids, another hybrid being (GT)₂₀-(8,4), that showed negligible changes in fluorescence intensity during 8 hour incubation in 10 % FBS-containing cell culture media (Figure 6). The stable hybrid CTC₃TC-(7,6) identified from our previous analysis of DNA coating displacement exhibited increase in fluorescence intensity, while varying levels of decrease in intensity were observed for the remaining hybrids (Figure 6). In addition, we observed negligible changes for absorbance and emission spectra of purified DNA-SWCNT hybrids after incubation in cell culture media with serum, an example of which is shown for the (-) (6,5) species at both room temperature and 37 °C (Figure S6). Specifically, a red shift (i.e., increase in wavelength) in E₁₁ emission peak was absent for several purified DNA-SWCNT hybrids and minimal red shifts of 1-3 nm (i.e., $\Delta E_{11} < 3.2$ meV) was observed for (7,3), (8,3), (7,6), (9,4), and (10,3) tubes. In comparison, DNA-SWCNT samples prepared from a synthetic nanotube mixture generally showed a spectral red shift (e.g., ΔE_{11} up to 7.7 meV with 6 hour incubation) [35] in serum-containing cell culture media due to electrostatic interactions of serum proteins and the phosphate backbone of DNA, which can cause nanotube aggregation [54]. Overall, negligible changes in absorbance spectra of purified DNA-SWCNT

hybrids were observed for incubation in cell culture media with serum (Figure S7), suggesting minimal nanotube aggregation.

However, several purified DNA-SWCNTs exposed to cell culture media without serum showed decrease in the E₁₁ absorbance values indicating the formation of nanotube aggregations and diminished nanotube stability (Figure S8). It is possible that the presence of serum proteins in cell culture media facilitates the dispersion stability of ordered DNA-SWCNT hybrids through forming a protective surface coating and preventing nanotube aggregation in cell culture media. In addition, the difference in pH of cell culture media with and without serum (i.e., pH 7.54 and 8.30, respectively) could possibly contribute to the different behaviors of purified DNA-SWCNT samples. Future studies on the effects of proteins and pH of cell culture media on the dispersion stability of purified DNA-SWCNTs will provide insights on the observed discrepancy in spectral stability of nanotubes in cell culture media with and without serum.

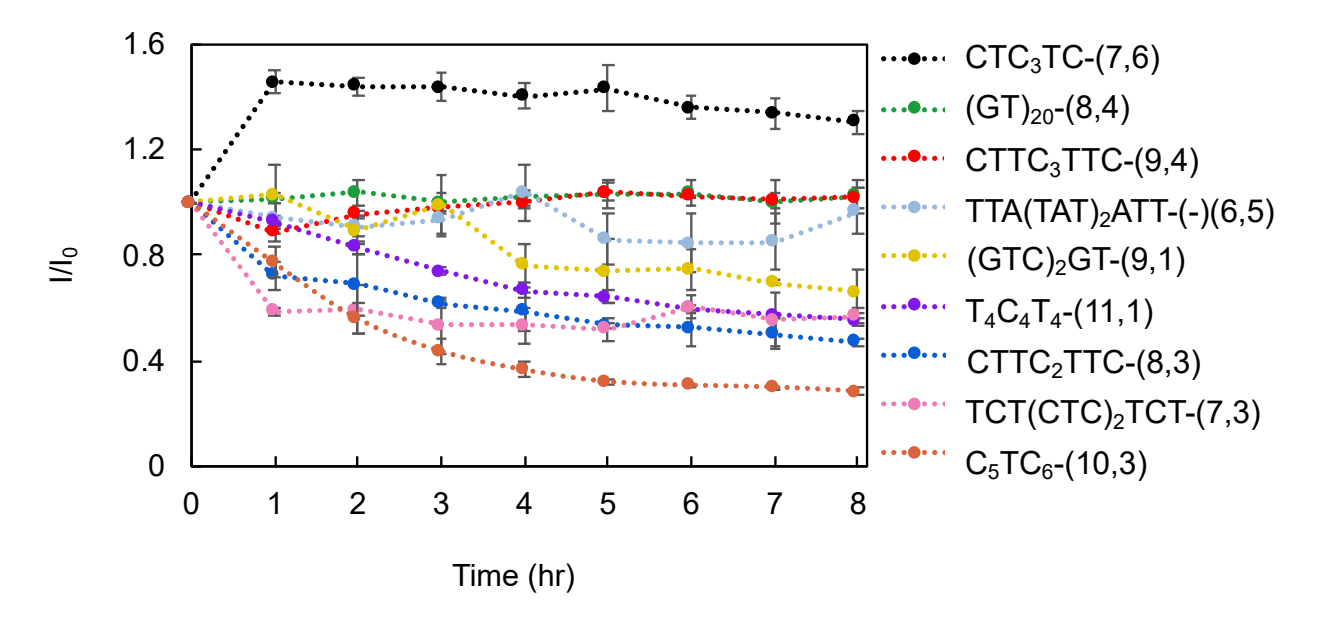


Figure 6. Intensity ratio at E₁₁ emission peak position of purified DNA-SWCNTs as a function of time in 10 % FBS-containing cell culture media at room temperature.

4. Conclusions

In summary, we have demonstrated the distinct complexation of pure-chirality SWCNTs and recognition DNA sequences in various aqueous environments, providing valuable insights for optical and physicochemical properties of many purified DNA-SWCNT hybrids that have not been achieved previously. Particularly, purified DNA-SWCNT hybrids showed a broad range of increase from 1.3-fold to 14.7-fold in nanotube PL intensity in the NIR with surfactant exchange. Moreover, the time constants obtained from fitting intensity increase in NIR fluorescence of purified DNA-SWCNT hybrids showed more than an order of magnitude difference ranging from 9 to 230 s, clearly showing distinct complexation of each DNA-SWCNT recognition pair. In addition, purified DNA-SWCNTs incubated in cell culture media with serum showed improved spectral stability compared to that of serum-free cell culture media. In this work, the potential of short DNA sequences in manipulating nanotubes was highlighted by a special hybrid CTC₃TC-(7,6), which could have potential application as a stable optical probe for detecting targeted molecular interactions in biology. It also provides new possibilities of creating unique DNA-SWCNT hybrids through the complexation of a pure-chirality SWCNT species, for example (7,6) tubes, with a DNA sequence of choice by combining the DNA/surfactant exchange and its reverse reaction, aided by methanol [55,56]. Our work provides a foundation for future studies involving carbon nanotube sorting and surface functionalization of pure-chirality SWCNTs to create multicolor, fluorescent molecular probes for applications such as bioimaging and biosensing.

Acknowledgments

We acknowledge support of Cleveland State University (CSU) Faculty Start-Up Funds, CSU Undergraduate Summer Research Award (USRA), and the National Science Foundation (CBET-1917513). We also acknowledge Dr. Ming Zheng for useful discussions.

Appendix A. Supplementary data

Supplementary data associated with this article can be found in the online version.

References

- [1] D.A. Heller, H. Jin, B.M. Martinez, D. Patel, B.M. Miller, T.-K. Yeung, et al., Multimodal optical sensing and analyte specificity using single-walled carbon nanotubes, Nat. Nanotechnol. 4 (2) (2009) 114–120.
- [2] S. Kruss, M.P. Landry, E. Vander Ende, B.M.A. Lima, N.F. Reuel, J. Zhang, et al., Neurotransmitter detection using corona phase molecular recognition on fluorescent single-walled carbon nanotube sensors, J. Am. Chem. Soc. 136 (2) (2014) 713–724.
- [3] K. Yum, J.-H. Ahn, T.P. McNicholas, P.W. Barone, B. Mu, J.-H. Kim, et al., Boronic acid library for selective, reversible near-infrared fluorescence quenching of surfactant suspended single-walled carbon nanotubes in response to glucose, ACS Nano 6 (1) (2012) 819–830.
- [4] J. Zhang, M.P. Landry, P.W. Barone, J.-H. Kim, S. Lin, Z.W. Ulissi, et al., Molecular recognition using corona phase complexes made of synthetic polymers adsorbed on carbon nanotubes, Nat. Nanotechnol. 8 (12) (2013) 959–968.
- [5] G. Bisker, J. Dong, H.D. Park, N.M. Iverson, J. Ahn, J.T. Nelson, et al., Protein-targeted corona phase molecular recognition, Nat. Commun. 7 (1) (2016) 10241.
- [6] N.M. Iverson, P.W. Barone, M. Shandell, L.J. Trudel, S. Sen, F. Sen, et al., In vivo biosensing via tissue-localizable near-infrared-fluorescent single-walled carbon nanotubes, Nat. Nanotechnol. 8 (11) (2013) 873–880.
- [7] X. Ma, L.-H. Zhang, L.-R. Wang, X. Xue, J.-H. Sun, Y. Wu, et al., Single-walled carbon nanotubes alter cytochrome c electron transfer and modulate mitochondrial function, ACS Nano 6 (12) (2012) 10486–10496.
- [8] T. V. Galassi, P. V. Jena, J. Shah, G. Ao, E. Molitor, Y. Bram, et al., An optical nanoreporter of endolysosomal lipid accumulation reveals enduring effects of diet on hepatic macrophages in vivo, Sci. Transl. Med. 10 (461) (2018), eaar2680.
- [9] N. Yang, X. Jiang, Nanocarbons for DNA sequencing: A review, Carbon 115 (2017) 293–311
- [10] M. Zheng, Sorting carbon nanotubes, Top. Curr. Chem. 375 (1) (2017) 13.
- [11] G. Ao, J.K. Streit, J.A. Fagan, M. Zheng, Differentiating left- and right-handed carbon nanotubes by DNA, J. Am. Chem. Soc. 138 (51) (2016) 16677–16685.

- [12] Y. Yomogida, T. Tanaka, M. Zhang, M. Yudasaka, X. Wei, H. Kataura, Industrial-scale separation of high-purity single-chirality single-wall carbon nanotubes for biological imaging, Nat. Commun. 7 (1) (2016) 12056.
- [13] M.T. Hasan, E. Campbell, O. Sizova, V. Lyle, G. Akkaraju, D.L. Kirkpatrick, et al., Multi-drug/gene NASH therapy delivery and selective hyperspectral NIR imaging using chirality-sorted single-walled carbon nanotubes, Cancers (Basel) 11 (8) (2019) 1175.
- [14] Y. Hu, H. Liu, C. Fang, C. Li, F. Xhyliu, H. Dysert, et al., Targeting of CD38 by the tumor suppressor miR-26a serves as a novel potential therapeutic agent in multiple myeloma, Cancer Res. (2020) canres. 1077.2019.
- [15] R.B. Weisman, S.M. Bachilo, Dependence of optical transition energies on structure for single-walled carbon nanotubes in aqueous suspension: An empirical Kataura plot, Nano Lett. 3 (9) (2003) 1235–1238.
- [16] S. Diao, G. Hong, J.T. Robinson, L. Jiao, A.L. Antaris, J.Z. Wu, et al., Chirality enriched (12, 1) and (11, 3) single-walled carbon nanotubes for biological imaging, J. Am. Chem. Soc. 134 (41) (2012) 16971–16974.
- [17] L. Ceppi, N.M. Bardhan, Y. Na, A. Siegel, N. Rajan, R. Fruscio, et al., Real-time single-walled carbon nanotube-based fluorescence imaging improves survival after debulking surgery in an ovarian cancer model, ACS Nano 13 (5) (2019) 5356–5365.
- [18] D. Roxbury, P. V Jena, R.M. Williams, B. Enyedi, P. Niethammer, S. Marcet, et al., Hyperspectral microscopy of near-infrared fluorescence enables 17-chirality carbon nanotube imaging, Sci. Rep. 5 (1) (2015) 14167.
- [19] C.W. Lin, R.B. Weisman, In vivo detection of single-walled carbon nanotubes: Progress and challenges, Nanomedicine 11 (22) (2016) 2885–2888.
- [20] J.P. Giraldo, M.P. Landry, S.Y. Kwak, R.M. Jain, M.H. Wong, N.M. Iverson, et al., A ratiometric sensor using single chirality near-infrared fluorescent carbon nanotubes: Application to in vivo monitoring, Small 11 (32) (2015) 3973–3984.
- [21] R.L. Pinals, D. Yang, A. Lui, W. Cao, M.P. Landry, Corona exchange dynamics on carbon nanotubes by multiplexed fluorescence monitoring, J. Am. Chem. Soc. 142 (3) (2020) 1254-1264.
- [22] A.L. Antaris, J.T. Robinson, O.K. Yaghi, G. Hong, S. Diao, R. Luong, et al., Ultra-low doses of chirality sorted (6, 5) carbon nanotubes for simultaneous tumor imaging and photothermal therapy, ACS Nano 7 (4) (2013) 3644–3652.
- [23] M. Kim, X. Wu, G. Ao, X. He, H. Kwon, N.F. Hartmann, et al., Mapping structure-property relationships of organic color centers, Chem 4 (9) (2018) 2180–2191.
- [24] A. Saha, B.J. Gifford, X. He, G. Ao, M. Zheng, H. Kataura, et al., Narrow-band single-photon emission through selective aryl functionalization of zigzag carbon nanotubes, Nat. Chem. 10 (11) (2018) 1089–1095.
- [25] X. He, N.F. Hartmann, X. Ma, Y. Kim, R. Ihly, J.L. Blackburn, et al., Tunable room-temperature single-photon emission at telecom wavelengths from sp³ defects in carbon nanotubes, Nat. Photonics 11 (9) (2017) 577–588.
- [26] C.-W. Lin, S.M. Bachilo, Y. Zheng, U. Tsedev, S. Huang, R.B. Weisman, et al., Creating fluorescent quantum defects in carbon nanotubes using hypochlorite and light, Nat. Commun. 10 (1) (2019) 2874.
- [27] Y. Yang, A. Shankar, T. Aryaksama, M. Zheng, A. Jagota, Quantification of DNA/SWCNT solvation differences by aqueous two-phase separation, Langmuir 34 (5) (2018) 1834-1843.
- [28] Y. Yang, M. Zheng, A. Jagota, Learning to predict single-wall carbon nanotube-recognition

- DNA sequences, npj Comput. Mater. 5 (1) (2019) 3.
- [29] G. Ao, C.Y. Khripin, M. Zheng, DNA-controlled partition of carbon nanotubes in polymer aqueous two-phase systems, J. Am. Chem. Soc. 136 (29) (2014) 10383–10392.
- [30] R.R. Johnson, A.T. Johnson, M.L. Klein, The nature of DNA-base-carbon-nanotube interactions, Small 6 (1) (2010) 31–34.
- [31] Y. Zheng, S.M. Bachilo, R.B. Weisman, Quenching of single-walled carbon nanotube fluorescence by dissolved oxygen reveals selective single-stranded DNA affinities, J. Phys. Chem. Lett. 8 (9) (2017) 1952–1955.
- [32] Y. Zheng, S.M. Bachilo, R.B. Weisman, Controlled patterning of carbon nanotube energy levels by covalent DNA functionalization, ACS Nano 13 (7) (2019) 8222–8228.
- [33] J.D. Harvey, P. V Jena, H.A. Baker, G.H. Zerze, R.M. Williams, T. V Galassi, et al., A carbon nanotube reporter of microRNA hybridization events in vivo, Nat. Biomed. Eng. 1 (4) (2017) 41.
- [34] T. V. Galassi, M. Antman-Passig, Z. Yaari, J. Jessurun, R.E. Schwartz, D.A. Heller, Longterm in vivo biocompatibility of single-walled carbon nanotubes, BioRxiv (2019) 869750.
- [35] M. Gravely, M.M. Safaee, D. Roxbury, Biomolecular functionalization of a nanomaterial to control stability and retention within live cells, Nano Lett. 19 (9) (2019) 6203-6212.
- [36] R.R. Johnson, A.T.C. Johnson, M.L. Klein, Probing the structure of DNA-carbon nanotube hybrids with molecular dynamics, Nano Lett. 8 (1) (2008) 69–75.
- [37] D. Roxbury, A. Jagota, J. Mittal, Sequence-specific self-stitching motif of short single-stranded DNA on a single-walled carbon nanotube, J. Am. Chem. Soc. 133 (34) (2011) 13545–13550.
- [38] A. Shankar, M. Zheng, A. Jagota, Energetic basis of single-wall carbon nanotube enantiomer recognition by single-stranded DNA, J. Phys. Chem. C 121 (32) (2017) 17479– 17487.
- [39] K.R. Hinkle, F.R. Phelan, Solvation of carbon nanoparticles in water/alcohol mixtures: Using molecular simulation to probe energetics, structure, and dynamics, J. Phys. Chem. C 121 (41) (2017) 22926–22938.
- [40] S. Iliafar, J. Mittal, D. Vezenov, A. Jagota, Interaction of single-stranded DNA with curved carbon nanotube is much stronger than with flat graphite, J. Am. Chem. Soc. 136 (37) (2014) 12947–12957.
- [41] Y. Zheng, S.M. Bachilo, R.B. Weisman, Enantiomers of single-wall carbon nanotubes show distinct coating displacement kinetics, J. Phys. Chem. Lett. 9 (2018) 3793–3797.
- [42] P. V Jena, M.M. Safaee, D.A. Heller, D. Roxbury, DNA–carbon nanotube complexation affinity and photoluminescence modulation are independent, ACS Appl. Mater. Interfaces 9 (25) (2017) 21397–21405.
- [43] F.F. Bergler, F. Schöppler, F.K. Brunecker, M. Hailman, T. Hertel, Fluorescence spectroscopy of gel-immobilized single-wall carbon nanotubes with microfluidic control of the surfactant environment, J. Phys. Chem. C 117 (25) (2013) 13318–13323.
- [44] D. Roxbury, X. Tu, M. Zheng, A. Jagota, Recognition ability of DNA for carbon nanotubes correlates with their binding affinity, Langmuir 27 (13) (2011) 8282–8293.
- [45] A. Shankar, J. Mittal, A. Jagota, Binding between DNA and carbon nanotubes strongly depends upon sequence and chirality, Langmuir 30 (11) (2014) 3176–3183.
- [46] Y. Kato, A. Inoue, Y. Niidome, N. Nakashima, Thermodynamics on soluble carbon nanotubes: How do DNA molecules replace surfactants on carbon nanotubes?, Sci. Rep. 2 (1) (2012) 733.

- [47] D. Roxbury, A. Jagota, J. Mittal, Structural characteristics of oligomeric DNA strands adsorbed onto single-walled carbon nanotubes, J. Phys. Chem. B 117 (1) (2012) 132–140.
- [48] G. Ao, M. Zheng, Preparation and separation of DNA-wrapped carbon nanotubes, Curr. Protoc. Chem. Biol. 7 (1) (2015) 43–51.
- [49] C.Y. Khripin, N. Arnold-Medabalimi, M. Zheng, Molecular-crowding-induced clustering of DNA-wrapped carbon nanotubes for facile length fractionation, ACS Nano 5 (10) (2011) 8258–8266.
- [50] M. Zheng, B.A. Diner, Solution redox chemistry of carbon nanotubes, J. Am. Chem. Soc. 126 (47) (2004) 15490–15494.
- [51] A.R.T. Nugraha, R. Saito, K. Sato, P.T. Araujo, A. Jorio, M.S. Dresselhaus, Dielectric constant model for environmental effects on the exciton energies of single wall carbon nanotubes, Appl. Phys. Lett. 97 (2010) 091905.
- [52] J.H. Choi, M.S. Strano, Solvatochromism in single-walled carbon nanotubes, Appl. Phys. Lett. 90 (2007) 223114.
- [53] D.A. Tsyboulski, E.L. Bakota, L.S. Witus, J.-D.R. Rocha, J.D. Hartgerink, R.B. Weisman, Self-assembling peptide coatings designed for highly luminescent suspension of single-walled carbon nanotubes, J. Am. Chem. Soc. 130 (50) (2008) 17134–17140.
- [54] X. Gong, A.K. Sharma, M.S. Strano, D. Mukhopadhyay, Selective assembly of DNA-conjugated single-walled carbon nanotubes from the vascular secretome, ACS Nano 8 (9) (2014) 9126–9136.
- [55] Y. Yang, A. Sharma, G. Noetinger, M. Zheng, A. Jagota, Pathway-dependent structures of DNA-wrapped carbon nanotubes: Direct sonication vs surfactant/DNA exchange, J. Phys. Chem. C 124 (16) (2020) 9045–9055.
- [56] J.K. Streit, J.A. Fagan, M. Zheng, A low energy route to DNA-wrapped carbon nanotubes via replacement of bile salt surfactants, Anal. Chem. 89 (19) (2017) 10496–10503.